Latest Improvements for CrIS Sensor Data Records

Yong Chen[1,2], Denis Tremblay[1,2], Flavio Iturbide-Sanchez[2], Joe Taylor[3], Xin Jin[1,2], Mark Esplin[4], and Dave Tobin[3]

Contact info: Yong.Chen@noaa.gov

[1]Global Science & Technology, Inc., Greenbelt, MD 20770, USA; [2]NOAA/NESDIS Center for Satellite Applications and Research, College Park, MD 20740, USA; [3]SSEC/University of Wisconsin-Madison, Madison, WI 53706, USA; [4]SDL/Utah State University, North Logan, UT 84341, USA

ITSC-XXII, poster 2p.03

Abstract

The Cross-track Infrared Sounder (CrIS) on board the Suomi National Polar-Orbiting Partnership (S-NPP) and NOAA-20 satellites have provided the hyperspectral infrared observations for profiling atmospheric temperature, moisture and greenhouse gases globally. CrIS is a well calibrated instrument through its excellent instrument design, well-conducted pre-launch and post-launch validations. The excellent performances of CrIS include noise below specification, high spectral and radiometric accuracy, high geolocation accuracy, as well as high long-term stability.

CrIS SDRs for S-NPP and NOAA-20 were transition to the validated status on February 20, 2014 and October 2, 2018, respectively. The operational CrIS SDR data quality is continuously being monitored and improved. Important algorithm improvements have been carried out recently, including the optimization of the spike detection and correction algorithm (operational implemented on October 3, 2018), optimization of the lunar intrusion detection algorithm (operational implemented on December 17, 2018), and the implementation of the polarization correction algorithm (planned operational implementation on 12/18/2019).

In this study, these specific areas of improvements in the CrIS SDR data quality are presented

Improved Lunar Intrusion (LI) Algorithm

Algorithm	Implementation Date	Code Main Feature	Threshold		
			LWIR	MWIR	SWIR
Original LI Detection Algorithm	From February 2012 until 17 December 2018	Assuming the first deep space (DS) spectrum in the moving window was non-contaminated as initial reference spectrum	0.1	0.1	0.1
New LI detection algorithm	17 December 2018 IDPS Block 2.1 Mx 4	Finding a non-contaminated spectrum in the moving window to use as the initial reference spectrum	0.003	0.003	0.0055
New LI detection algorithm with improved LI thresholds	10 May 2019 IDPS Block 2.1 Mx 5	Finding a non-contaminated spectrum in the moving window to use as the initial reference spectrum	0.003	0.004	0.0095

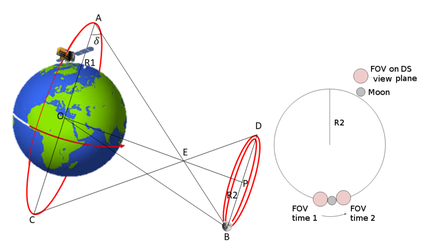

Scheme of the lunar intrusions in CrIS deep space view plane in which the Moon's position falls on the circle to derive the number of successive DS view affected by a single lunar intrusion event.

The maximum number of scans with successive DS views that is possible in a single LI event, N_{LI}, is about 10.3.

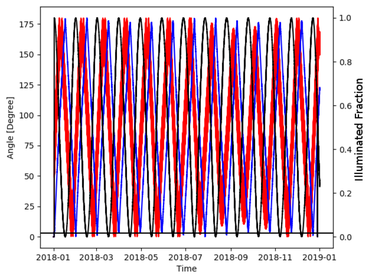

Moon in CrIS field of regard during 2018. Red curve-separation angle between the CrIS space view and the Moon vector; Blue curve-separation angle between the Sun and the Moon vectors as lunar phase; Black curve-Moon illuminated fraction; and Black line-CrIS FOR angle (3.3º).

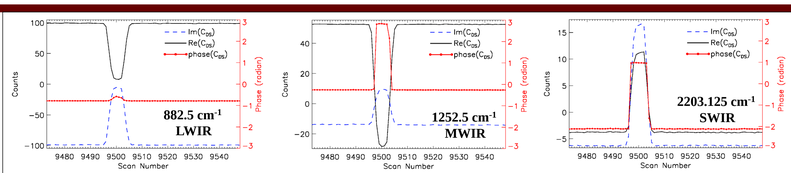

The time evolution of the real part and imaginary part of the DS spectrum C_{DS}, as well as its phase (red curve with solid circle) for S-NPP CrIS FOV 1 reverse mirror sweep direction on 25 February 2018 during a lunar intrusion event

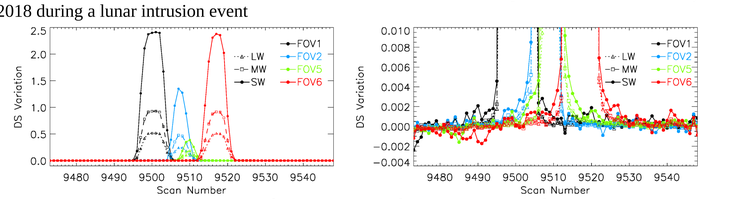

Time series S-NPP CrIS reverse interferometer sweep direction DS spectral variations at FOVs 1, 2, 5, and 6 on 25 February 2018 during a lunar intrusion event. Determination of the three bands LI_{lim} values.

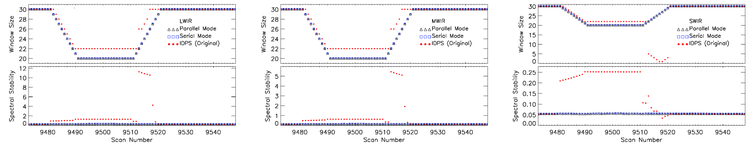

DS moving window size and spectral stability as a function of scan lines. Serial mode (blue square) can be treated as truth since DS moving window does not need to be reestablished and the first DS spectrum is contamination-free. IDPS (red filled cycle) is referred to the original operational algorithm before 17 December 2108 with lunar intrusion threshold as 0.1 for all three bands, while parallel mode (black triangle) is for the new algorithm. Both serial mode and parallel mode are using new threshold values as 0.003, 0.004, and 0.0095 for three CrIS bands, respectively.

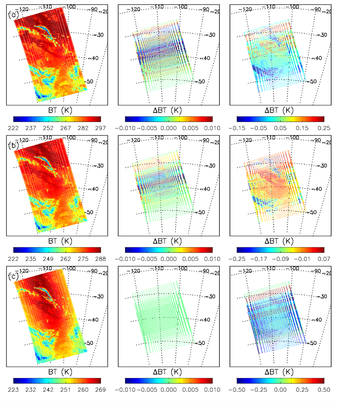

Brightness temperatures (BT) from serial run as references (left column), and BT differences for these two parallel runs compared to the serial run (middle column: BT difference between the parallel run and the serial run using new LI detection algorithm, and last column: BT difference between the original and new LI detection algorithms) for these FOVs affected by lunar intrusion at three wavenumbers: (a) 900.0 cm^{-1}, (b) 1252.50 cm^{-1}, and (c) 2203.125cm^{-1}, respectively, on a lunar intrusion event on 25 February 2018.

Polarization Correction Algorithm

- As the SSM rotates, the mirror polarization couples with the polarization of the CrIS intrument and produce a small radiometric offset which is FOV, FOR and Band dependent. This small but detectable offset need to be corrected in the earth radiance
- Polarization correction parameters were derived from the on-orbit pitch maneuver data
- All the polarization correction related parameters were in CrIS processing control table (PCT)

$$E_p = \frac{L_{ES}\,p_r\,p_t\cos(2\delta_{ES}-\alpha) + B_{SSM}\,p_r\,p_t[\cos(2\theta_{DS})-\cos(2\theta_{ES})] - L_{ES}\,p_r\,p_t\cos(2\theta_{ICT}) - L_{ES}\frac{B_{SSM}}{L_{ICT}}\,p_r\,p_t[\cos(\theta_{DS})-\cos(\theta_{ICT})]}{1+p_r\,p_t\cos(2\theta_{DS})}$$
$$= \frac{L_{ES}\,p_r\,p_t\cos(2\theta_{ES}) + B_{SSM}\,p_r\,p_t[\cos(2\theta_{DS})-\cos(2\theta_{ES})] - L_{ES}\,p_r\,p_t\cos(2\theta_{DS})}{1+p_r\,p_t\cos(2\theta_{DS})}$$
$$= p_r\,p_t\frac{L_{ES}\cos(2\theta_{ES}) + B_{SSM}[\cos(2\theta_{DS})-\cos(2\theta_{ES})] - L_{ES}\cos(2\theta_{DS})}{1+p_r\,p_t\cos(2\theta_{DS})}$$
$$= p_r\,p_t\frac{(L_{ES}-B_{SSM})[\cos(2\theta_{ES})-\cos(2\theta_{DS})]}{1+p_r\,p_t\cos(2\theta_{DS})}$$
$$= p_r\,p_t\frac{(L_{ES}-B_{SSM})[\cos(2(\delta_{ES}-\alpha))-\cos(2(\delta_{DS}-\alpha))]}{1+p_r\,p_t\cos(2(\delta_{DS}-\alpha))}$$

$\boldsymbol{p_r p_t}$: the combined polarization of SSM (p_r) and sensor (p_t), is spectral and FOV dependent

$\boldsymbol{\alpha}$: the effective polarizer angle of the sensor, is band and FOV dependent

$\boldsymbol{\delta}$: the effective polarization angle of the scene mirror, is FOV dependent for DS, ICT. For ES, it is also FOR dependent

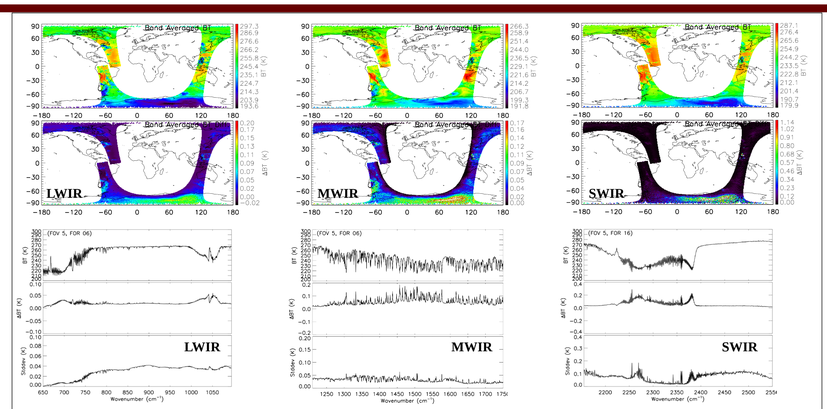

Polarization correction impact on radiance (brightness temperature) for NOAA-20 three CrIS bands (off/on)

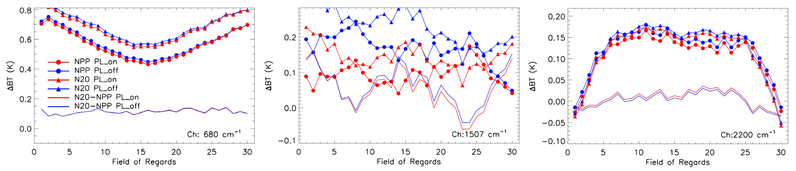

- Polarization correction reduces the brightness temperature difference between observation and simulation
- Polarization correction makes the brightness temperature difference more symmetric around nadir FORs
- The polarization correction improvement is small for these clear warm ocean scenes, but clearly in the right direction

Spike Detection and Correction Algorithm

- Detecting spikes through interferogram asymmetry. SWIR is most affected due to the smallest detector current)
- Correction is achieved by subtracting a modeled spike from the observed interferogram
- Least-squares fit used to determine position and amplitude of spike
- Shape of spike is simply the impulse response of the analog electronics and the digital signal processing
- Improving these earth view radiance spectra from invalid due to the larger imaginary radiance exceeding thresholds to valid

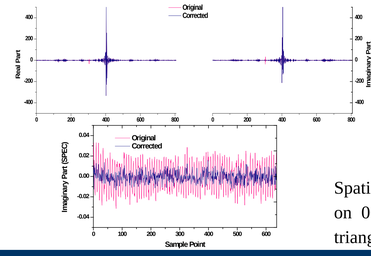

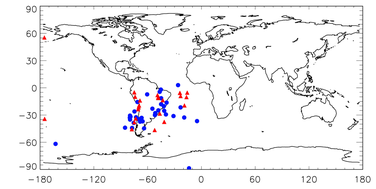

Spatial distribution of spikes detected and corrected pixels on 06/05/2019. Blue cycles are for Earth Scenes, Red triangles are for ICT and DS views.

Conclusion

- The lunar intrusion detection algorithm effectively removes the deep space (DS) spectra contaminated by lunar contribution in the calibration DS sliding window, improves the quality of the ES radiances during lunar intrusion events
- Polarization correction algorithm includes correcting the calibration bias due to the instrument polarization effect for the earth radiances
- Spike detection and correction algorithm reduces the distorted earth view radiance spectra by correcting the spike in the raw interferograms

References

- Chen, Y., D. Tremblay, L. Wang, and F. Iturbidesanchez (2019), Improved Lunar intrusion detection algorithm for the CrIS Sensor Data Record, IEEE, trans. Geosci and remote sensing, doi:10.1109/TGRS.2019.2944003
- Taylor, J., and et al. (2017), Current CrIS calibration activities at UW-SSEC, the 21st International TOVS Study Conference, Darmstadt, Germany, 29 November to 5 December 2017
- Esplin M., B. Esplin, and D. Scott (2017), Removing radiation-induced spikes from Fourier transform data, Conference on Characterization and Radiometric Calibration or Remote Sensing, Logon, Utah